EPJ Web of Conferences **192**, 00004 (2018) https://doi.org/10.1051/epjconf/201819200004
QCD@Work 2018

Single-top and top-antitop cross sections

Nikolaos Kidonakis[1,*]

[1]Department of Physics, Kennesaw State University, Kennesaw, GA 30144, USA

Abstract. I present high-order calculations, including soft-gluon corrections, for single-top and top-antitop production cross sections and differential distributions. For single-top production, results are presented for the three different channels in the Standard Model, for associated production with a charged Higgs, and for processes involving anomalous couplings. For top-antitop pair production, total cross sections and top-quark transverse-momentum and rapidity distributions are presented for various LHC energies.

1 Introduction

Higher-order soft-gluon corrections have been calculated through N^{3}LO for top-quark production via various processes; see Ref. [1] for a review. Here I present the latest results for t-channel and s-channel single-top production, tW and tH^- production, tZ production via anomalous couplings, and $t\bar{t}$ production. For all these processes QCD corrections are very significant and are dominated by soft-gluon corrections.

I calculate and resum these soft corrections at next-to-next-to-leading logarithm (NNLL) accuracy for the double-differential cross section, which is then used to calculate top-quark transverse-momentum and rapidity distributions and total cross sections. Finite-order expansions at approximate NNLO (aNNLO) and approximate N^{3}LO (aN^{3}LO), matched to exact results, provide the best predictions for these quantities.

We calculate soft-gluon corrections for partonic processes of the form

$$f_1(p_1) + f_2(p_2) \to t(p_t) + X$$

and we define $s = (p_1 + p_2)^2$, $t = (p_1 - p_t)^2$, $u = (p_2 - p_t)^2$, and $s_4 = s + t + u - \sum m^2$. At partonic threshold $s_4 \to 0$. The nth-order soft-gluon corrections appear as $\left[\ln^k(s_4/m_t^2)/s_4\right]_+$ where $k \le 2n-1$.

Moments of the partonic cross section, $\hat{\sigma}(N) = \int (ds_4/s)\, e^{-Ns_4/s} \hat{\sigma}(s_4)$, can be written in factorized form

$$\sigma^{f_1 f_2 \to tX}(N,\epsilon) = H_{IL}^{f_1 f_2 \to tX}(\alpha_s(\mu_R))\, S_{LI}^{f_1 f_2 \to tX}\left(\frac{m_t}{N\mu_F}, \alpha_s(\mu_R)\right) \prod J_{\rm in}(N,\mu_F,\epsilon) \prod J_{\rm out}(N,\mu_F,\epsilon)$$

in $4-\epsilon$ dimensions, where $H_{IL}^{f_1 f_2 \to tX}$ is a hard function and $S_{LI}^{f_1 f_2 \to tX}$ is a soft-gluon function. $S_{LI}^{f_1 f_2 \to tX}$ satisfies the renormalization group equation

$$\left(\mu\frac{\partial}{\partial\mu} + \beta(g_s)\frac{\partial}{\partial g_s}\right) S_{LI}^{f_1 f_2 \to tX} = -(\Gamma_S^\dagger)_{LK}^{f_1 f_2 \to tX} S_{KI}^{f_1 f_2 \to tX} - S_{LK}^{f_1 f_2 \to tX} (\Gamma_S)_{KI}^{f_1 f_2 \to tX}$$

*e-mail: nkidonak@kennesaw.edu

where the soft anomalous dimension $\Gamma_S^{f_1 f_2 \to tX}$ controls the evolution of the soft function, giving the exponentiation of logarithms of N. To achieve NNLL accuracy we need to calculate the relevant soft anomalous dimensions at two loops.

2 Single-top production

We now provide results for single-top production in the t-channel, s-channel, and via tW production. Fixed-order results for these processes are known at NNLO for the t-channel [2–4] and s-channel [5], and at NLO for tW production [6]. Here we provide results with soft-gluon corrections at aNNLO for t- and s-channel production [7], and at aN^{3}LO for tW production [8]; these results are obtained from NNLL resummation [7–9]. We use MMHT2014 NNLO pdf [10].

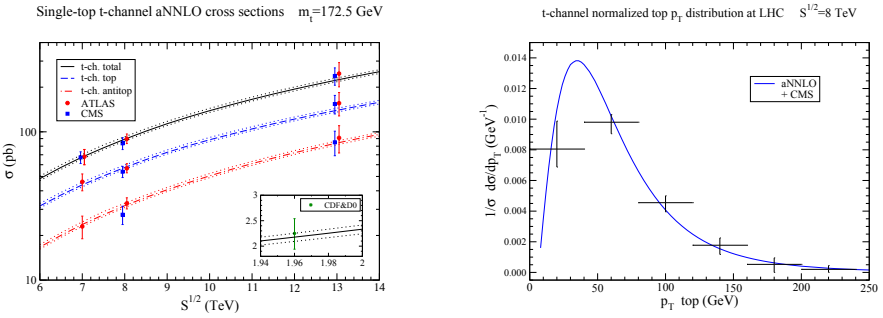

Figure 1. (Left) Single-top t-channel aNNLO cross sections compared with CMS and ATLAS data at 7 TeV [12, 13], 8 TeV [14, 15], and 13 TeV [16, 17], and with CDF and D0 combined data at 1.96 TeV [18]. (Right) Top-quark aNNLO normalized p_T distributions in t-channel production at 8 TeV compared to CMS [19] data.

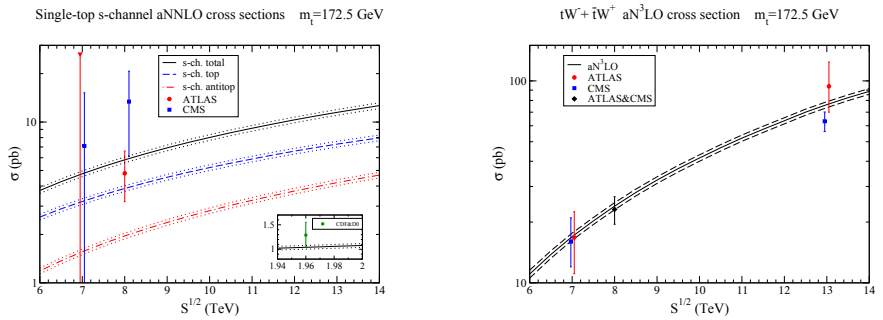

Figure 2. (Left) Single-top s-channel aNNLO cross sections compared to ATLAS and CMS data at 7 TeV [20, 21] and 8 TeV [21, 22], and to CDF and D0 combined data [23] at 1.96 TeV. (Right) aN^{3}LO cross sections for tW production compared to ATLAS and CMS data at 7 TeV [24, 25], 8 TeV [26], and 13 TeV [27, 28].

We begin with t-channel production at aNNLO. In the left plot of Fig. 1 we display total t-channel cross sections as functions of collider energy at the LHC and (inset) at the Tevatron.

Results are given for the single-top cross section, the single-antitop cross section, and their sum. We observe very good agreement of the aNNLO theory curves [7, 11] with all available data from the LHC and the Tevatron at various energies. The right plot of Fig. 1 shows the aNNLO normalized top-quark p_T distributions at 8 TeV LHC energy, which describe the corresponding data from CMS [19] quite well.

We continue with s-channel production at aNNLO. In the left plot of Fig. 2 we show cross sections for single-top and single-antitop s-channel production, and their sum, as functions of energy at the LHC and (inset) at the Tevatron. We again observe very good agreement of the aNNLO theory curves [7, 11] with available data at LHC and Tevatron energies.

We next discuss tW production at aN^{3}LO. In the right plot of Fig. 2 we show the total $tW^-+\bar{t}W^+$ cross section as a function of LHC energy. Very good agreement is observed between the aN^{3}LO results [8, 11] and the data at 7, 8, and 13 TeV energies.

3 tH^- production

We continue with tH^- production in the MSSM or other two-Higgs-doublet models [29]. We use MMHT2014 NNLO pdf [10] for our numerical results.

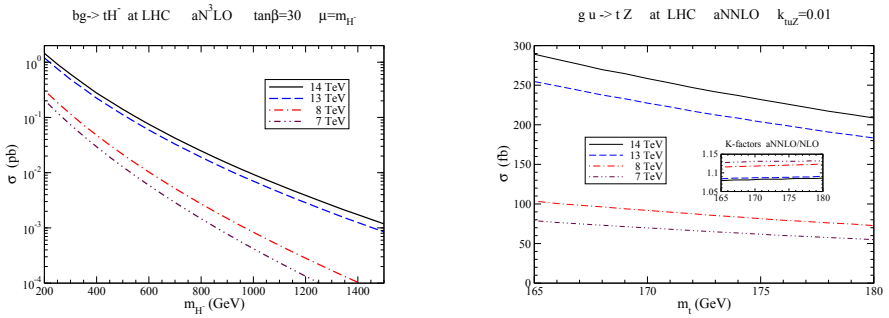

Figure 3. (Left) aN^{3}LO cross sections for tH^- production. (Right) aNNLO cross sections for tZ production via anomalous couplings.

In the left plot of Fig. 3 we show the aN^{3}LO total cross section for tH^- production [11] as a function of charged-Higgs mass at LHC energies of 7, 8, 13, and 14 TeV. We use $\tan\beta = 30$. The soft-gluon corrections are large for this process. Top-quark p_T and rapidity distributions in this process have also been presented in [29].

4 tZ production via anomalous couplings

Next, we discuss soft-gluon corrections in tZ production in models with anomalous t-q-Z couplings [30, 31]. The NLO corrections for this process were calculated in Ref. [32]. The complete NLO corrections are very well approximated by the soft-gluon corrections at that order.

We use CT14 pdf [33] for our numerical results in this process. In the right plot of Fig. 3 we plot the aNNLO total cross section for tZ production as a function of top-quark mass at LHC energies of 7, 8, 13, and 14 TeV.

The K-factors shown in the inset plot show that the aNNLO corrections are large and significantly enhance the NLO cross section, especially at lower energies. This is important

in providing theoretical input to experimental limits on the couplings [34, 35]. Top-quark differential distributions in this process have been presented in Ref. [31].

Similar results have more recently been presented for $t\gamma$ production via anomalous couplings in Ref. [36].

5 Top-antitop pair production

Finally, we discuss top-antitop pair production [37, 38]. The soft anomalous dimensions are 2×2 matrices for the $q\bar{q} \to t\bar{t}$ channel, and 3×3 matrices for the $gg \to t\bar{t}$ channel.

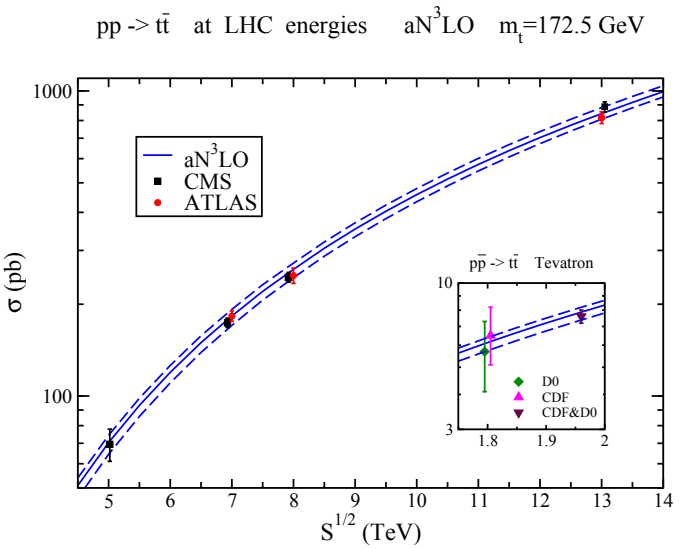

Figure 4. Top-antitop aN^{3}LO cross sections compared with CMS data at 5.02 TeV [41] and with ATLAS and CMS data at 7 TeV [42, 43], 8 TeV [43, 44], and 13 TeV [45, 46] LHC energies. The inset shows the aN^{3}LO cross section compared with CDF [47] and D0 [48] data at 1.8 TeV, and CDF&D0 combined data [49] at 1.96 TeV Tevatron energy.

At one loop for $q\bar{q} \to t\bar{t}$, the elements of the $\Gamma_S^{q\bar{q}\to t\bar{t}}$ matrix in an s-channel singlet-octet color basis are

$$\Gamma_{11}^{q\bar{q}\to t\bar{t}\,(1)} = \Gamma_{\rm cusp}^{(1)}\,, \quad \Gamma_{12}^{q\bar{q}\to t\bar{t}\,(1)} = \frac{C_F}{C_A}\ln\left(\frac{t_1}{u_1}\right), \quad \Gamma_{21}^{q\bar{q}\to t\bar{t}\,(1)} = 2\ln\left(\frac{t_1}{u_1}\right),$$
$$\Gamma_{22}^{q\bar{q}\to t\bar{t}\,(1)} = \left(1-\frac{C_A}{2C_F}\right)\Gamma_{\rm cusp}^{(1)} + 4C_F\ln\left(\frac{t_1}{u_1}\right) - \frac{C_A}{2}\left[1+\ln\left(\frac{sm_t^2t_1^2}{u_1^4}\right)\right].$$

At two loops for $q\bar{q} \to t\bar{t}$, the elements of the $\Gamma_S^{q\bar{q}\to t\bar{t}}$ matrix are

$$\Gamma_{11}^{q\bar{q}\to t\bar{t}\,(2)} = \Gamma_{\rm cusp}^{(2)}\,, \quad \Gamma_{12}^{q\bar{q}\to t\bar{t}\,(2)} = \left(\frac{K}{2}-\frac{C_A}{2}N_{2l}\right)\Gamma_{12}^{q\bar{q}\to t\bar{t}\,(1)},$$
$$\Gamma_{21}^{q\bar{q}\to t\bar{t}\,(2)} = \left(\frac{K}{2}+\frac{C_A}{2}N_{2l}\right)\Gamma_{21}^{q\bar{q}\to t\bar{t}\,(1)},$$
$$\Gamma_{22}^{q\bar{q}\to t\bar{t}\,(2)} = \frac{K}{2}\Gamma_{22}^{q\bar{q}\to t\bar{t}\,(1)} + \left(1-\frac{C_A}{2C_F}\right)\left(\Gamma_{\rm cusp}^{(2)}-\frac{K}{2}\Gamma_{\rm cusp}^{(1)}\right).$$

See also Ref. [1] for more details. Here $\Gamma_{\rm cusp}$ is the cusp anomalous dimension [39].

The soft-gluon corrections are large and they are excellent approximations to the complete corrections at both NLO and NNLO. The additional corrections at aN^{3}LO provide further significant enhancements and must be included for precision physics. Another approach for the aN^{3}LO corrections has appeared recently in Ref. [40].

In our numerical results below we use the MMHT2014 NNLO pdf [10]. The total top-antitop cross sections at aN^{3}LO [38] are shown in Fig. 4 and compared with data at Tevatron and LHC energies. We find remarkable agreement between theory and data at all energies.

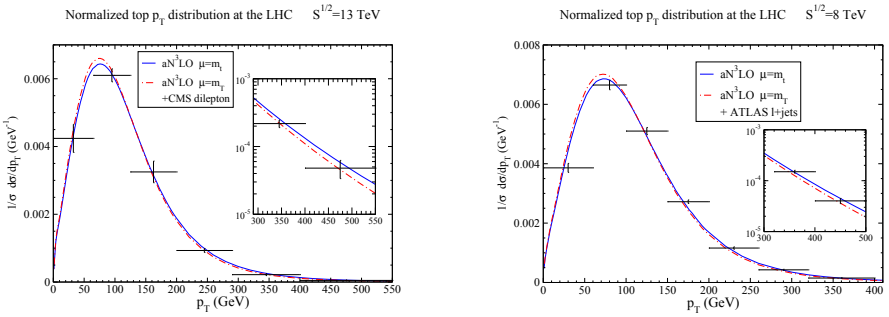

Figure 5. aN^{3}LO top-quark normalized p_T distributions (left) at 13 TeV energy compared with CMS [50] data and (right) at 8 TeV energy compared with ATLAS [51] data.

The aN^{3}LO top-quark normalized p_T distributions in $t\bar{t}$ production are shown in Fig. 5 at 13 TeV (left plot) and 8 TeV (right plot) and compared with CMS and ATLAS data respectively. We find excellent agreement of the theoretical predictions with the data.

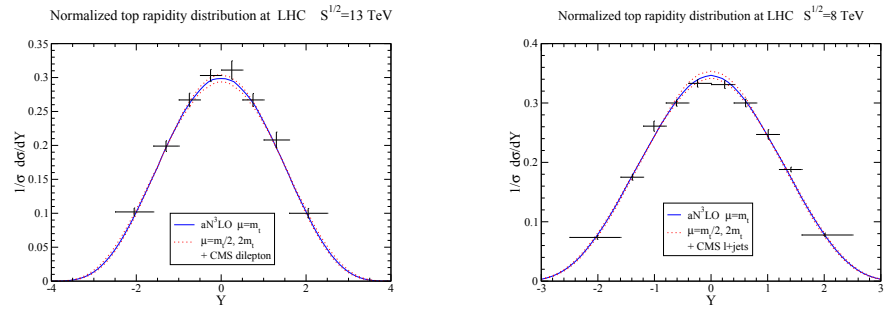

Figure 6. Top-quark aN^{3}LO normalized rapidity distribution at (left) 13 TeV energy compared with CMS data [50] and (right) 8 TeV energy compared with CMS data [52].

The aN^{3}LO top-quark normalized rapidity distributions in $t\bar{t}$ production are shown in Fig. 6 at 13 TeV (left plot) and 8 TeV (right plot) and compared with CMS data. Again, we find that the theory curves provide an excellent description of the data.

6 Summary

We have discussed cross sections and distributions for various top-quark production processes. Soft-gluon corrections are important in all cases. We have shown results for t-channel and s-channel single-top production at aNNLO, tW production at aN^{3}LO, tH^- production at aN^{3}LO, tZ production via anomalous couplings at aNNLO, and $t\bar{t}$ production at aN^{3}LO. We find excellent agreement with available collider data. The higher-order corrections are very significant and need to be included for better theoretical predictions.

Acknowledgments

This material is based upon work supported by the National Science Foundation under Grant No. PHY 1519606.

References

[1] N. Kidonakis, Int. J. Mod. Phys. A **33**, 1830021 (2018) [arXiv:1806.03336 [hep-ph]].
[2] M. Brucherseifer, F. Caola, and K. Melnikov, Phys. Lett. B **736**, 58 (2014) [arXiv:1404.7116 [hep-ph]].
[3] E.L. Berger, J. Gao, C.-P. Yuan, and H.X. Zhu, Phys. Rev. D **94**, 071501 (2016) [arXiv:1606.08463 [hep-ph]].
[4] E.L. Berger, J. Gao, and H.X. Zhu, JHEP **1711**, 158 (2017) [arXiv:1708.09405 [hep-ph]].
[5] Z. Liu and J. Gao, arXiv:1807.03835 [hep-ph].
[6] S.H. Zhu, Phys. Lett. B **524**, 283 (2002) [Erratum: *ibid.* **537**, 351 (2002)] [hep-ph/0109269].
[7] N. Kidonakis, Phys. Rev. D **81**, 054028 (2010) [arXiv:1001.5034 [hep-ph]]; **83**, 091503(R) (2011) [arXiv:1103.2792 [hep-ph]]; **88**, 031504(R) (2013) [arXiv:1306.3592 [hep-ph]]; **93**, 054022 (2016) [arXiv:1510.06361 [hep-ph]].
[8] N. Kidonakis, Phys. Rev. D **96**, 034014 (2017) [arXiv:1612.06426 [hep-ph]]; in *Proceedings of DPF 2017*, eConf C170731 [arXiv:1709.06975 [hep-ph]].
[9] N. Kidonakis, Phys. Rev. D **82**, 054018 (2010) [arXiv:1005.4451 [hep-ph]].
[10] L.A. Harland-Lang, A.D. Martin, P. Molytinski, and R.S. Thorne, Eur. Phys. J. C **75**, 204 (2015) [arXiv:1412.3989 [hep-ph]].
[11] N. Kidonakis, in *Proceedings of CIPANP2018* [arXiv:1808.02934 [hep-ph]].
[12] CMS Collab., JHEP **1212**, 035 (2012) [arXiv:1209.4533 [hep-ex]].
[13] ATLAS Collab., Phys. Rev. D **90**, 112006 (2014) [arXiv:1406.7844 [hep-ex]].
[14] CMS Collab., JHEP **1406**, 090 (2014) [arXiv:1403.7366 [hep-ex]].
[15] ATLAS Collab., Eur. Phys. J. C **77**, 531 (2017) [arXiv:1702.02859 [hep-ex]].
[16] ATLAS Collab., JHEP **1704**, 086 (2017) [arXiv:1609.03920 [hep-ex]].
[17] CMS Collab., Phys. Lett. B **772**, 752 (2017) [arXiv:1610.00678 [hep-ex]].
[18] CDF and D0 Collab., Phys. Rev. Lett. **115**, 152003 (2015) [arXiv:1503.05027 [hep-ex]].
[19] CMS Collab., CMS-PAS-TOP-14-004.
[20] ATLAS Collab., ATLAS-CONF-2011-118.
[21] CMS Collab., JHEP **1609**, 027 (2016) [arXiv:1603.02555 [hep-ex]].
[22] ATLAS Collab., Phys. Lett. B **756**, 228 (2016) [arXiv:1511.05980 [hep-ex]].
[23] CDF and D0 Collab., Phys. Rev. Lett. **112**, 231803 (2014) [arXiv:1402.5126 [hep-ex]].
[24] ATLAS Collab., Phys. Lett. B **716**, 142 (2012) [arXiv:1205.5764 [hep-ex]].
[25] CMS Collab., Phys. Rev. Lett. **110**, 022003 (2013) [arXiv:1209.3489 [hep-ex]].

[26] ATLAS and CMS Collab., ATLAS-CONF-2016-023, CMS-PAS-TOP-15-019.
[27] ATLAS Collab., JHEP **1801**, 063 (2018) [arXiv:1612.07231 [hep-ex]].
[28] CMS Collab., arXiv:1805.07399 [hep-ex].
[29] N. Kidonakis, JHEP **0505**, 011 (2005) [hep-ph/0412422]; Phys. Rev. D **94**, 014010 (2016) [arXiv:1605.00622 [hep-ph]].
[30] A. Belyaev and N. Kidonakis, Phys. Rev. D **65**, 037501 (2002) [hep-ph/0102072]; N. Kidonakis and A. Belyaev, JHEP **0312**, 004 (2003) [hep-ph/0310299].
[31] N. Kidonakis, Phys. Rev. D **97**, 034028 (2018) [arXiv:1712.01144 [hep-ph]].
[32] B.H. Li, Y. Zhang, C.S. Li, J. Gao, and H.X. Zhu, Phys. Rev. D **83**, 114049 (2011) [arXiv:1103.5122 [hep-ph]].
[33] S. Dulat, T.-J. Hou, J. Gao, M. Guzzi, J. Huston, P. Nadolsky, J. Pumplin, C. Schmidt, D. Stump, and C.-P. Yuan, Phys. Rev. D **93**, 033006 (2016) [arXiv:1506.07443 [hep-ph]].
[34] CMS Collaboration, JHEP **1707**, 003 (2017) [arXiv:1702.01404 [hep-ex]].
[35] ATLAS Collaboration, ATLAS-CONF-2017-070.
[36] M. Forslund and N. Kidonakis, arXiv:1808.09014 [hep-ph].
[37] N. Kidonakis, Phys. Rev. D **82**, 114030 (2010) [arXiv:1009.4935 [hep-ph]]; in *Physics of Heavy Quarks and Hadrons, HQ2013* [arXiv:1311.0283 [hep-ph]].
[38] N. Kidonakis, Phys. Rev. D **90**, 014006 (2014) [arXiv:1405.7046 [hep-ph]]; **91**, 031501(R) (2015) [arXiv:1411.2633 [hep-ph]]; **91**, 071502(R) (2015) [arXiv:1501.01581 [hep-ph]].
[39] N. Kidonakis, Phys. Rev. Lett. **102**, 232003 (2009) [arXiv:0903.2561 [hep-ph]]; Int. J. Mod. Phys. A **31**, 1650076 (2016) [arXiv:1601.01666 [hep-ph]].
[40] J. Piclum and C. Schwinn, JHEP **1803**, 164 (2018) [arXiv:1801.05788 [hep-ph]].
[41] CMS Collab., JHEP **1803**, 115 (2018) [arXiv:1711.03143 [hep-ex]].
[42] ATLAS Collab., Eur. Phys. J. C **74**, 3109 (2014) [Addendum: *ibid.* **76**, 642 (2016)] [arXiv:1406.5375 [hep-ex]].
[43] CMS Collab., JHEP **1608**, 029 (2016) [arXiv:1603.02303 [hep-ex]].
[44] ATLAS Collab., Eur. Phys. J. C **78**, 487 (2018) [arXiv:1712.06857 [hep-ex]].
[45] ATLAS Collab., Phys. Lett. B **761**, 136 (2016) [Erratum: *ibid.* **772**, 879 (2017)] [arXiv:1606.02699 [hep-ex]].
[46] CMS Collab., JHEP **1709**, 051 (2017) [arXiv:1701.06228 [hep-ex]].
[47] CDF Collab., Phys. Rev. D **64**, 032002 (2001) [Erratum: *ibid.* **67**, 119901 (2003)] [hep-ex/0101036].
[48] D0 Collab., Phys. Rev. D **67**, 012004 (2003) [hep-ex/0205019].
[49] CDF and D0 Collab., Phys. Rev. D **89**, 072001 (2014) [arXiv:1309.7570 [hep-ex]].
[50] CMS Collab., JHEP **1804**, 060 (2018) [arXiv:1708.07638 [hep-ex]].
[51] ATLAS Collab., Eur. Phys. J. C **76**, 538 (2016) [arXiv:1511.04716 [hep-ex]].
[52] CMS Collab., Eur. Phys. J. C **75**, 542 (2015) [arXiv:1505.04480 [hep-ex]].